DALTON
FULL PAPER

Synthesis, structure, and interconversion of chiral rhenium oxygen- and sulfur-bound sulfoxide complexes of formula [(η^5-C_5H_5)-Re(NO)(PPh_3)(OS(Me)R)]$^+$ X$^-$; diastereoselective oxidations of coordinated methyl alkyl sulfides†

Michael Otto,[a] **Brian J. Boone,**[b] **Atta M. Arif**[b] **and J. A. Gladysz** *[a]

[a] *Institut für Organische Chemie, Universität Erlangen-Nürnberg, Henkestrasse 42, 91054 Erlangen, Germany*
[b] *Department of Chemistry, University of Utah, Salt Lake City, Utah 84112, USA*

Received 28th November 2000, Accepted 13th February 2001
First published as an Advance Article on the web 23rd March 2001

Reactions of the chiral chlorobenzene complex [(η^5-C_5H_5)Re(NO)(PPh_3)(ClC_6H_5)]$^+$$BF_4^-$ ($\mathbf{1}^+$ BF_4^-) and alkyl methyl sulfoxides O=S(Me)R (R = **a**, Me; **b**, Et; **c**, *i*-Pr or **d**, *t*-Bu), at −15 °C gave the oxygen-bound sulfoxide complexes [(η^5-C_5H_5)Re(NO)(PPh_3)(**O**=S(Me)R)]$^+$ BF_4^- (**2a**–**2d**$^+$$BF_4^-$; 94–56%). Above 0 °C, **2a**–**2d**$^+$$BF_4^-$ rearrange to sulfur-bound linkage isomers [(η^5-C_5H_5)Re(NO)(PPh_3)(**S**(=O)(Me)R)]$^+$$BF_4^-$ (**3a**–**3d**$^+$$BF_4^-$; 96–20%). The triflate salts **2c**,**2d**$^+$TfO$^-$ and **3b**,**3c**$^+$TfO$^-$ are analogously prepared from (η^5-C_5H_5)Re(NO)(PPh_3)(OTf). Complexes **2b**–**2d**$^+$X$^-$ and **3b**–**3d**$^+$X$^-$ can exist as two Re, S configurational diastereomers. Stereochemistry is assigned from reactions of (*S*)- or (*R*)-$\mathbf{1}^+$$BF_4^-$ with enantiomerically enriched sulfoxides (*R*)-**b**–**d**, and a crystal structure of ($S_{Re}R_S$,$R_{Re}S_S$)-**2d**$^+$TfO$^-$·0.5CH_2Cl_2. Relative diastereomer stabilities, and the basis for the divergent kinetic and thermodynamic oxygen/sulfur binding selectivities, are analysed. The alkyl methyl sulfide complexes [(η^5-C_5H_5)Re(NO)(PPh_3)(S(Me)R)]$^+$ X$^-$ and dimethyldioxirane react (acetone, −20 °C) to give **3a**–**3d**$^+$X$^-$. Diastereoselectivities (**3b**–**3d**$^+$X$^-$) are fair to good. However, some overoxidation to Ph_3P=O occurs, lowering yields.

Introduction

Many compounds with sulfur stereocenters occur naturally, and others play important roles as chiral auxiliaries or catalysts in asymmetric organic synthesis.[1] Thus, the enantioselective oxidation of organic sulfides to sulfoxides has received considerable attention.[2–6] We were attracted approximately a decade ago to the potential use of chiral transition metal Lewis acids as platforms for such oxidations. We noted the possibility that the thermodynamic binding affinities of sulfur-bound sulfoxide ligands might be lower than those of the corresponding sulfides, due to the electronegative oxo (=O) moiety. Hence, a successful stoichiometric oxidation of a metal sulfide complex might be modified to run catalytically (*e.g.* the displacement of a product ligand by an educt ligand would be energetically favorable).

In our first efforts we studied the binding of methyl alkyl sulfide ligands to the chiral rhenium Lewis acid [(η^5-C_5H_5)-Re(NO)(PPh_3)]$^+$ **I**, as well as an achiral sulfoxide ligand, DMSO.[7] The feasibility of sulfoxide/sulfide ligand exchange was demonstrated,[7] and later novel base-induced rearrangements of coordinated DMSO[8] and diallyl or related sulfides were explored.[9] Importantly, lone pairs on atoms ligating to **I** commonly show enhanced basicity or nucleophilicity.[10] Thus, we anticipated that rhenium-bound sulfides would react faster than free sulfides with electrophilic oxidizing agents, another important requirement for catalysis. Soon after we commenced our studies the need for independently prepared authentic samples of sulfoxide complexes became apparent.

In this paper we report high yield syntheses of oxygen- and sulfur-bound methyl alkyl sulfoxide complexes of formula [(η^5-C_5H_5)Re(NO)(PPh_3)(OS(Me)R)]$^+$X$^-$. The spectroscopic and structural properties of these linkage isomers, each of which can exist as two rhenium/sulfur configurational diastereomers (R ≠ Me), are analysed in detail. Preliminary data on the oxidation of the corresponding sulfide complexes are also described. Very similar work with chiral ruthenium Lewis acids was simultaneously undertaken by Schenk and co-workers.[5,11] Their data have appeared before ours, aided by superior oxidation chemistry as described in the Discussion section.

Results

1 Syntheses of sulfoxide complexes

The substitution-labile, racemic chlorobenzene complex [(η^5-C_5H_5)Re(NO)(PPh_3)(ClC_6H_5)]$^+$$BF_4^-$ ($\mathbf{1}^+$$BF_4^-$), which is a mixture of several isomeric species, was generated at −45 °C in chlorobenzene as previously described.[12] As shown in Scheme 1, *ca.* two equivalents of the racemic sulfoxides O=S(Me)R (R = **a**, Me; **b**, Et; **c**, *i*-Pr or **d**, *t*-Bu) were added. The samples were kept at −15 °C for several hours. Low temperature precipitations gave 85–99 : 15–1 mixtures[13] of the oxygen-bound sulfoxide complexes [(η^5-C_5H_5)Re(NO)(PPh_3)(O=S(MeR)]$^+$-BF_4^- (**2a**–**2d**$^+$$BF_4^-$) and the sulfur-bound sulfoxide complexes [(η^5-C_5H_5)Re(NO)(PPh_3)(S=O)(Me)R)]$^+$$BF_4^-$ (**3a**–**3d**$^+$$BF_4^-$) as orange powders in 56–94% yields. Both diastereomers of **2b**–**2d**$^+$$BF_4^-$ were detected.[14] Ratios varied somewhat in different experiments (Scheme 1 and footnotes), and configurations were assigned as described below.

Analogous reactions were monitored by ^{31}P NMR. In all cases, the oxygen-bound complexes $\mathbf{2}^+$$BF_4^-$ were the dominant kinetic products. When **2a**–**2c**$^+$$BF_4^-$ were warmed to room temperature clean isomerization to sulfur-bound complexes **3a**–**3c**$^+$$BF_4^-$ occurred. However, the sterically more congested S-*t*-Bu species **2d**$^+$$BF_4^-$ gave mainly decomposition products, and only modest yields of **3d**$^+$$BF_4^-$. A second series of preparative reactions were conducted in which the samples were kept at room temperature for several hours. Work-ups gave pure **3a**–**3d**$^+$$BF_4^-$ as yellow powders in 86–96 (**a**–**c**) to 20% (**d**) yields, as summarized in Scheme 1. Diastereomer ratios differed from

---

† Electronic supplementary information (ESI) available: preparative and characterization data for complexes **2**–**5**$^+$X$^-$, full crystallographic data for ($S_{Re}R_S$·$R_{Re}S_S$)-**2d**$^+$TfO$^-$·0.5CH_2Cl_2. See http://www.rsc.org/suppdata/dt/b0/b009533h/

DOI: 10.1039/b009533h

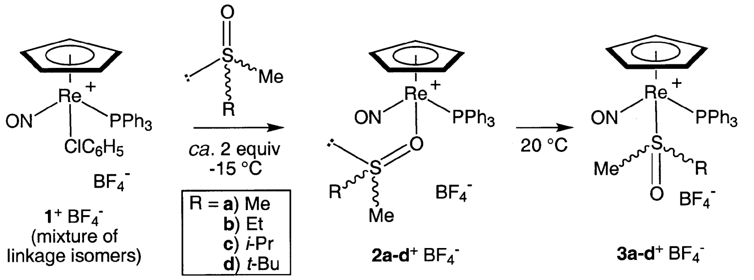

	Oxygen-bound sulfoxides $(\mathbf{2a\text{-}d}^+\ BF_4^-)^a$				Sulfur-bound sulfoxides $(\mathbf{3a\text{-}d}^+\ BF_4^-)^a$	
	Ligand Yield (%)	$\mathbf{2}^+/\mathbf{3}^+$ Ratio	Diastereomer Ratio $R_{Re}S_S,S_{Re}R_S$/ $R_{Re}R_S,S_{Re}S_S$		Ligand Yield (%)	Diastereomer Ratio $S_{Re}R_S,R_{Re}S_S$/ $S_{Re}S_S,R_{Re}R_S$
a	84	90:10	-----	**a**	86^b	-----
b	56^c	91:9	19:81	**b**	93	50:50
	-----	-----	-----		$(93)^d$	(45:55)
c	85^e	85:15	83:17	**c**	96	43:57
	$(63)^d$	(85:15)	(70:30)		$(75)^d$	(53:47)
d	94^f	99:1	50:50	**d**	20	<1:>99
	$(83)^d$	(>99:<1)	(98:2)	-----	-----	-----

[a] Data are for two separate sets of preparative reactions (low temperature workups for $\mathbf{2a\text{-}d}^+$ BF_4^-, ambient tempeature workups for $\mathbf{3a\text{-}d}^+$ BF_4^-). [b] This yield is from the procedure in ref. 7. [c] A second similar experiment gave a 74% yield and 64:36 and 37:63 mixtures of isomers. [d] Data in parentheses are for the corresponding triflate salts, analogously prepared from $(\eta^5\text{-}C_5H_5)Re(NO)(PPh_3)(OTf)$; see text. [e] A second similar experiment gave a 78% yield and 85:15 and 52:48 mixtures of isomers. [f] A second similar experiment gave a 99% yield and 98:2 and 67:33 mixtures of isomers.

Scheme 1 Syntheses of sulfoxide complexes.

those of $\mathbf{2b}$–$\mathbf{2d}^+BF_4^-$,[14b] and possible reasons (apart from the intrinsic variability of precipitative work-ups) are discussed below. The DMSO complex $\mathbf{3a}^+BF_4^-$ was prepared earlier (from a dichloromethane complex similar to $\mathbf{1}^+BF_4^-$), and full characterization, including a crystal structure, has been reported.[8]

As summarized in the Experimental section and Table 1, $\mathbf{2a}$–$\mathbf{2d}^+BF_4^-$ and $\mathbf{3b}$–$\mathbf{3d}^+BF_4^-$ were characterized by IR and NMR (^1H, ^{13}C, ^{31}P) spectroscopy. Microanalyses were obtained for $\mathbf{3b}$–$\mathbf{3d}^+BF_4^-$. Oxygen-bound complexes $\mathbf{2}^+BF_4^-$ gave lower IR ν_{NO} values (1668–1685 cm^{-1}) than the sulfur-bound complexes $\mathbf{3}^+BF_4^-$ (1717–1722 cm^{-1}). This suggests that the oxygen-bound ligands have lower π acidities.[16] The ^{31}P NMR chemical shifts of $\mathbf{2}^+BF_4^-$ (δ 18.2–20.0) were markedly downfield from those of $\mathbf{3}^+BF_4^-$ (δ 9.0–12.6). The cyclopentadienyl, S*Me*, and S*R* ^1H and ^{13}C NMR resonances of $\mathbf{2}^+BF_4^-$ were also downfield from those of $\mathbf{3}^+BF_4^-$.

We sought similar data for selected triflate (O_3SCF_3) salts. As summarized in Scheme 1, reactions of the triflate complex $(\eta^5\text{-}C_5H_5)Re(NO)(PPh_3)(OTf)$ **4**[17] with sulfoxides **c**,**d** at 0 °C gave $\mathbf{2c},\mathbf{2d}^+TfO^-$ in 63–83% yields. The diastereomer ratios did not match those of the analogous tetrafluoroborate salts, and possible factors are discussed below. Reactions of **4** with **b**,**c** at ambient temperature gave $\mathbf{3b},\mathbf{3c}^+TfO^-$ in 75–93% yields. NMR spectra were essentially identical with those of the tetrafluoroborate salts. However, IR spectra showed triflate anion bands (1264 vs, 1224 m, 1154 s, 1031 s cm^{-1}) in place of tetrafluoroborate anion bands (1111 s, 1094 vs, 1055 vs, 998 s cm^{-1}). The absence of the latter allowed the ν_{SO} bands of sulfur-bound complexes $\mathbf{3b},\mathbf{3c}^+TfO^-$ to be located (1113–1121 s cm^{-1}). The wavenumbers were higher than those of the oxygen-bound complexes $\mathbf{2c},\mathbf{2d}^+X^-$ (885–891 m cm^{-1}), in accord with literature trends.[18]

2 Structures of sulfoxide complexes

We sought to assign configurations to the diastereomeric oxygen- and sulfur-bound sulfoxide complexes. The chlorobenzene complex $\mathbf{1}^+BF_4^-$ is easily generated in enantiomerically pure form, and undergoes substitution with retention of configuration at rhenium,[12] as verified crystallographically in the case of diallyl sulfide.[9a] Thus, isopropyl methyl sulfoxide (**c**) that was enriched in the *R* enantiomer (34% enantiomeric excess (ee) or 67 : 33 *R*/*S*) was prepared by Kagan's method.[4a] As shown in Scheme 2 (top), it was added to (*S*)-$\mathbf{1}^+BF_4^-$ (1.3 : 1.0 mol ratio) in an NMR tube at −45 °C. The sample was warmed to −10 °C, and the formation of $\mathbf{2c}^+BF_4^-$ monitored by ^{31}P NMR. At 93% conversion resonances at δ 18.2 and 18.9 were present in a 68 : 32 ratio.[13] Hence, they were assigned to $(R_{Re}R_S)$-$\mathbf{2c}^+BF_4^-$ and $(R_{Re}S_S)$-$\mathbf{2c}^+BF_4^-$,[14b] respectively. The sample was warmed to 25 °C. When isomerization was 83% complete resonances at δ 10.0 and 8.0 were present in a 78 : 22 ratio. These were assigned to $(S_{Re}S_S)$-$\mathbf{3c}^+BF_4^-$ and $(S_{Re}R_S)$-$\mathbf{3c}^+BF_4^-$.[14b]

The enriched isopropyl methyl sulfoxide was similarly added to complex (*R*)-$\mathbf{1}^+BF_4^-$ (1.1 : 1.0 mol ratio), and the reaction monitored by ^{31}P NMR at −10 °C (Scheme 2, bottom). At 80% conversion, resonances at δ 18.2 and 18.9 were present in a 30 : 70 ratio, and were assigned to $(S_{Re}S_S)$-$\mathbf{2c}^+BF_4^-$ and $(S_{Re}R_S)$-$\mathbf{2c}^+BF_4^-$, respectively. The sample was warmed to 25 °C. When isomerization was 74% complete resonances at δ 10.0 and 8.0 were present in a 40 : 60 ratio, and were assigned to $(R_{Re}R_S)$-$\mathbf{3c}^+BF_4^-$ and $(R_{Re}S_S)$-$\mathbf{3c}^+BF_4^-$.[14b] Note that if isomerization were complete the diastereomer ratios before and after isomerization would (in the absence of processes involving epimerization or dissociation/racemization) be identical. The decrease in the percentage of the major diastereomer in this experiment, coupled with the increase in the previous experiment, could be a simple consequence of slightly faster isomerizations of $(R_{Re}R_S)$-$\mathbf{2c}^+BF_4^-$ and $(S_{Re}S_S)$-$\mathbf{2c}^+BF_4^-$.

In a similar experiment, *t*-butyl methyl sulfoxide (**d**) that was enriched in the *R* enantiomer (38% ee or 69 : 31 *R*/*S*)[4a] was added to complex (*S*)-$\mathbf{1}^+BF_4^-$ (1.1 : 1.0 mol ratio) at −45 °C. The formation of $\mathbf{2d}^+BF_4^-$ was monitored by ^{31}P NMR at 0 °C. At 95% conversion resonances at δ 18.9 and 19.3 were present in

Table 1 NMR Characterization of rhenium sulfoxide complexes[a]

Complex	^{1}H NMR[b]	^{13}C-{^{1}H} NMR[c]	^{31}P-{^{1}H} NMR[d]
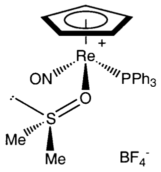 **2a**$^+$ BF_4^-	7.65–7.20 (m, $3C_6H_5$) 5.48 (s, C_5H_5) 2.55 (s, SCH_3) 2.44 (s, $SC'H_3$)[e]	Ph at: 133.6 (d, J = 11.1, *o*) 131.6 (d, J = 55.4, *p*) 131.2 (d, J = 2.0, *i*) 128.9 (d, J = 11.1, *m*) 91.6 (s, C_5H_5) 38.9 (s, SCH_3) 36.4 (s, $SC'H_3$)[e]	20.0[e]
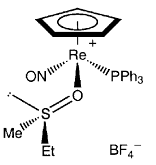 (*RS,SR*)-**2b**$^+$ BF_4^-	7.60–7.22 (m, $3C_6H_5$) 5.48 (s, C_5H_5) 3.03 (q, J = 7.2, SCH_2) 2.52 (s, SCH_3) 1.04 (t, J = 7.2, CH_2CH_3)[f]	Ph at: 133.4 (d, J = 8.4, *o*) 131.9 (d, J = 54.1, *i*) 131.3 (d, J = 2.4, *p*) 129.1 (d, J = 11.0, *m*) 91.6 (s, C_5H_5) 44.1 (s, SCH_2) 34.3 (s, SCH_3) 5.2 (s, CH_2CH_3)[f]	18.3 (s)[f]
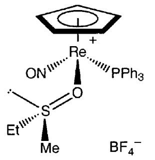 (*RR,SS*)-**2b**$^+$ BF_4^-	7.60–7.22 (m, $3C_6H_5$) 5.47 (s, C_5H_5) 3.40 (q, J = 6.9, SCH_2) 2.49 (s, SCH_3) 0.95 (t, J = 7.3, CH_2CH_3)[f]	Ph at: 133.6 (d, J = 11.1, *o*) 131.8 (d, J = 54.3, *i*) 131.4 (d, J = 2.7, *p*) 129.0 (d, J = 10.5, *m*) 91.7 (d, J = 2.0, C_5H_5) 46.4 (s, SCH_2) 32.2 (s, SCH_3) 5.0 (s, CH_2CH_3)[f]	18.6 (s) [f]
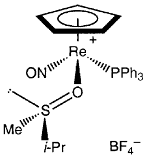 (*RS,SR*)-**2c**$^+$ BF_4^-	7.70–7.21 (m, $3C_6H_5$) 5.46 (s, C_5H_5) 3.04 (h, J = 6.9, SCH) 2.46 (s, SCH_3) 1.05 (d, J = 6.6, $CHCH_3$) 0.82 (d, J = 6.9, $CHC'H_3$)[f]	Ph at: 133.61 (d, J = 11.1, *o*) 131.9 (d, J = 54.4, *i*) 131.4 (d, J = 2.0, *p*) 129.1 (d, J = 11.1, *m*) 91.80 (s, C_5H_5) 52.6 (s, SCH) 29.0 (s, SCH_3) 14.8 (s, $CHCH_3$) 13.9 (s, $CHC'H_3$)[f]	18.9 (s)[f]
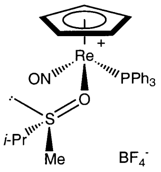 (*RR,SS*)-**2c**$^+$ BF_4^-	7.70–7.21 (m, $3C_6H_5$) 5.49 (s, C_5H_5) 3.03 (h, J = 7.0, SCH) 2.44 (s, SCH_3) 1.04 (d, J = 6.9, $CHCH_3$) 0.89 (d, J = 6.9, $CHC'H_3$)[f]	Ph at: 133.64 (d, J = 10.1, *o*) 132.1 (d, J = 54.4, *i*) 131.3 (d, J = 2.0, *p*) 129.0 (d, J = 11.1, *m*) 91.75 (s, C_5H_5) 50.2 (s, SCH) 30.2 (s, SCH_3) 15.2 (s, $CHCH_3$) 15.1 (s, $CHC'H_3$)[f]	18.2 (s)[f]
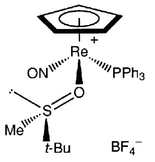 (*RS,SR*)-**2d**$^+$ BF_4^-	7.42–7.58 (m, 9H of $3C_6H_5$) 7.22–7.35 (m, 6H of $3C_6H_5$) 5.45 (s, C_5H_5) 2.47 (s, SCH_3) 1.01 (s, CCH_3)[f]	Ph at: 133.5 (d, J = 11.1, *o*) 132.6 (d, J = 55.4, *i*) 131.7 (d, J = 2.0, *p*) 129.11 (d, J = 11.1, *m*) 91.82 (s, C_5H_5) 58.4 (s, CCH_3) 27.3 (s, SCH_3) 22.0 (s, CCH_3)[f]	19.3 (s)[f]
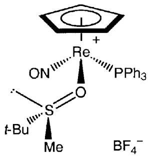 (*RR,SS*)-**2d**$^+$ BF_4^-	7.42–7.58 (m, 9H of $3C_6H_5$) 7.22–7.35 (m, 6H of $3C_6H_5$) 5.48 (s, C_5H_5) 2.45 (s, SCH_3) 1.05 (s, CCH_3)[f]	Ph at: 133.6 (d, J = 11.1, *o*) 132.4 (d, J = 52.4, *i*) 131.5 (d, J = 2.0, *p*) 129.09 (d, J = 11.1, *m*) 91.77 (s, C_5H_5) 56.6 (s, CCH_3) 29.0 (s, SCH_3) 22.2 (s, CCH_3)[f]	18.9 (s)[f]
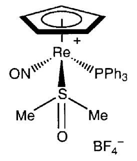 **3a**$^+$ BF_4^-	7.57–7.42 (m, $3C_6H_5$) 5.67 (s, C_5H_5) 3.53 (s, SCH_3) 3.31 (s, $SC'H_3$)[g]	Ph at: 133.9 (d, J = 11.0, *o*) 132.8 (d, J = 57.6, *p*) 132.1 (d, J = 2.2, *i*) 129.5 (d, J = 11.3, *m*) 94.4 (s, C_5H_5) 56.2 (s, SCH_3) 52.8 (s, $SC'H_3$)[g]	9.3 (s)[g]

Table 1 (*Contd.*)

Complex	^{1}H NMR[b]	^{13}C-{^{1}H} NMR[c]	^{31}P-{^{1}H} NMR[d]
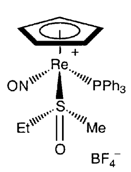 (SR,RS)-**3b**$^+$ BF_4^-	7.61–7.38 (m, 3C_6H_5) 5.68 (s, C_5H_5) 3.54 (m, SC*H*H′) 3.46 (dq, *J* = 7.1, SCH*H′*) 3.19 (s, SCH_3) 1.25 (t, *J* = 7.2, CH_2CH_3)	Ph at: 133.9 (d, *J* = 11.0, *o*) 132.7 (d, *J* = 57.4, *i*) 132.0 (d, *J* = 2.6, *p*) 129.5 (d, *J* = 11.1, *m*) 94.1 (d, *J* = 1.1, C_5H_5) 61.0 (s, SCH_2) 50.0 (s, SCH_3) 6.91 (s, CH_2CH_3)	9.3 (s)
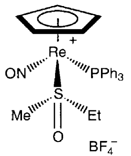 (SS,RR)-**3b**$^+$ BF_4^-	7.61–7.38 (m, 3C_6H_5) 5.66 (s, C_5H_5) 3.54 (m, SC*H*H′) 3.34 (dq, *J* = 7.4, SCH*H′*) 3.08 (s, SCH_3) 1.19 (t, *J* = 7.2, CH_2CH_3)	Ph at: 134.0 (d, *J* = 10.9, *o*) 132.9 (d, *J* = 57.6, *i*) 132.1 (d, *J* = 2.6, *p*) 129.6 (d, *J* = 11.0, *m*) 94.4 (d, *J* = 1.0, C_5H_5) 61.6 (s, SCH_2) 47.0 (s, SCH_3) 6.94 (s, CH_2CH_3)	9.5 (s)
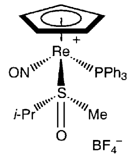 (SR,RS)-**3c**$^+$ BF_4^-	7.62–7.24 (m, 3C_6H_5) 5.62 (s, C_5H_5) 3.61 (h, *J* = 6.9, SCH) 2.29 (s, SCH_3) 1.35 (d, *J* = 6.7, $CHCH_3$) 1.31 (d, *J* = 6.7, $CHC'H_3$)	Ph at: 134.3 (d, *J* = 10.7, *o*) 133.2 (d, *J* = 57.9, *i*) 132.3 (d, *J* = 2.7, *p*) 129.8 (d, *J* = 10.9, *m*) 94.9 (d, *J* = 1.1, C_5H_5) 68.5 (s, SCH) 37.2 (s, SCH_3) 17.4 (s, $CHCH_3$) 14.1 (s, $CHC'H_3$)	8.0 (s)
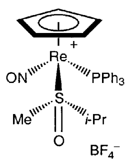 (SS,RR)-**3c**$^+$ BF_4^-	7.62–7.24 (m, 3C_6H_5) 5.67 (s, C_5H_5) 3.49 (h, *J* = 6.7, SCH) 3.00 (s, SCH_3) 1.38 (d, *J* = 6.7, $CHCH_3$) 1.33 (d, *J* = 6.7, $CHC'H_3$)	Ph at: 133.8 (d, *J* = 11.0, *o*) 132.6 (d, *J* = 57.9, *i*) 132.0 (d, *J* = 2.7, *p*) 129.4 (d, *J* = 11.2, *m*) 94.1 (d, *J* = 1.1, C_5H_5) 67.1 (s, SCH) 46.9 (s, SCH_3) 16.9 (s, $CHCH_3$) 15.8 (s, $CHC'H_3$)	10.0 (s)
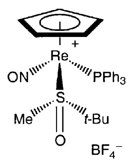 (SS,RR)-**3d**$^+$ BF_4^-	7.50–7.64 (m, 3C_6H_5) 6.02 (s, C_5H_5) 3.05 (s, SCH_3) 2.08 (s, CCH_3)	Ph at: 134.5 (d, *J* = 12.0, *o*) 132.3 (d, *J* = 2.7, *p*)[h] 129.8 (d, *J* = 11.2, *m*) 95.2 (d, *J* = 1.3, C_5H_5) 72.5 (s, CCH_3) 46.1 (s, SCH_3) 24.2 (s, CCH_3)	12.6 (s)

[a] Spectra are recorded in CD_2Cl_2 at ambient probe temperature unless noted. [b] At 300 MHz (δ) and referenced to internal $Si(CH_3)_4$. All couplings (Hz) are to ^{1}H. [c] At 75 MHz and referenced to CD_2Cl_2 (δ 53.8). All couplings (Hz) are to ^{31}P. Assignment of phenyl carbon resonances are made as described in footnote c of Table 1 in ref. 15. [d] At 121 MHz and referenced to external 85% H_3PO_4. [e] Spectrum recorded at −40 °C. [f] Spectrum recorded at −30 °C. [g] Data previously reported in Table 1 in ref. 7. [h] *ipso* carbon not observed.

a 66 : 34 ratio. Hence, they were assigned to ($R_{Re}R_S$)-**2d**$^+BF_4^-$ and ($R_{Re}S_S$)-**2d**$^+BF_4^-$, respectively. The enriched *t*-butyl methyl sulfoxide was similarly added to (*R*)-**1**$^+BF_4^-$, and the sample warmed to ambient temperature. At 67% conversion resonances at δ 18.9 and 19.3 were present in a 29 : 71 ratio, and assigned to ($S_{Re}S_S$)-**2d**$^+BF_4^-$ and ($S_{Re}R_S$)-**2d**$^+BF_4^-$, respectively. Consistent with data above, the preceding two samples underwent only partial isomerization to **3d**$^+BF_4^-$. This required heating to 60 °C, and gave concurrent decomposition. However, the major diastereomers at the lowest conversions were opposite. Thus, resonances could be assigned to ($S_{Re}S_S$)- or ($R_{Re}R_S$)-**3d**$^+BF_4^-$ (δ 11.0) and ($S_{Re}R_S$)- or ($R_{Re}S_S$)-**3d**$^+BF_4^-$ (δ 10.9).[14b]

Finally, ethyl methyl sulfoxide (**b**) that was enriched in the *R* enantiomer (69 : 31 *R*/*S*, 38% ee)[4a] was similarly added to complex (*S*)-**1**$^+BF_4^-$ (1.0 : 1.0 mol ratio) −45 °C. The formation of **2b**$^+BF_4^-$ was monitored by ^{31}P NMR. At 77% conversion (4.5 h, 0 °C) resonances at δ 19.1 and 18.9 were present in a 69 : 31 ratio,[19a] and assigned to ($R_{Re}R_S$)-**2b**$^+BF_4^-$ and ($R_{Re}S_S$)-**2b**$^+BF_4^-$, respectively. The sample was warmed to 25 °C. At 92% conversion the δ 9.8 and 9.6 resonances were present in a 67 : 33 ratio,[19b] and assigned to ($S_{Re}S_S$)-**3b**$^+BF_4^-$ and ($S_{Re}R_S$)-**3b**$^+BF_4^-$. This sequence was repeated with (*R*)-**1**$^+BF_4^-$. At 73% conversion (4.2 h, 0 °C) resonances at δ 19.1 and 18.9 were present in a 37 : 63 ratio, and assigned to ($S_{Re}S_S$)-**2b**$^+BF_4^-$ and ($S_{Re}R_S$)-**2b**$^+BF_4^-$, respectively.[19c] The sample was warmed to 25 °C. At 89% conversion resonances at δ 9.8 and 9.6 were present in a 34 : 66 ratio,[19d] and assigned to ($R_{Re}R_S$)-**3b**$^+BF_4^-$ and ($R_{Re}S_S$)-**3b**$^+BF_4^-$. Plots of the concentrations of **1**$^+BF_4^-$ and the various sulfoxide complex isomers *versus* time and temperature for all of these experiments (or equivalent ones) are given elsewhere.[20]

Configurations were assigned to diastereomers of the triflate salts **2c**,**2d**$^+$TfO$^-$ and **3b**,**3c**$^+$TfO$^-$ based upon the NMR relationships established for the tetrafluoroborate salts. The racemic oxygen-bound *t*-butyl methyl sulfoxide complex **2d**$^+$TfO$^-$, which was isolated as a 98 : 2 mixture of $R_{Re}S_S$,$S_{Re}R_S$/$R_{Re}R_S$,$S_{Re}S_S$ diastereomers (Scheme 1), was crystallized. This gave the diastereomerically pure solvate ($R_{Re}S_S$,$S_{Re}R_S$)-**2d**$^+$TfO$^-$·0.5CH_2Cl_2 (confirmed by NMR as the major diastereomer). X-Ray data were collected as summarized in the Experimental section. Refinement gave the structures in Fig. 1. Key bond lengths, bond angles, and torsion angles are summarized in Table 2. The crystal structure confirms (1) the linkage isomer assignment, (2) the configurational assignments made

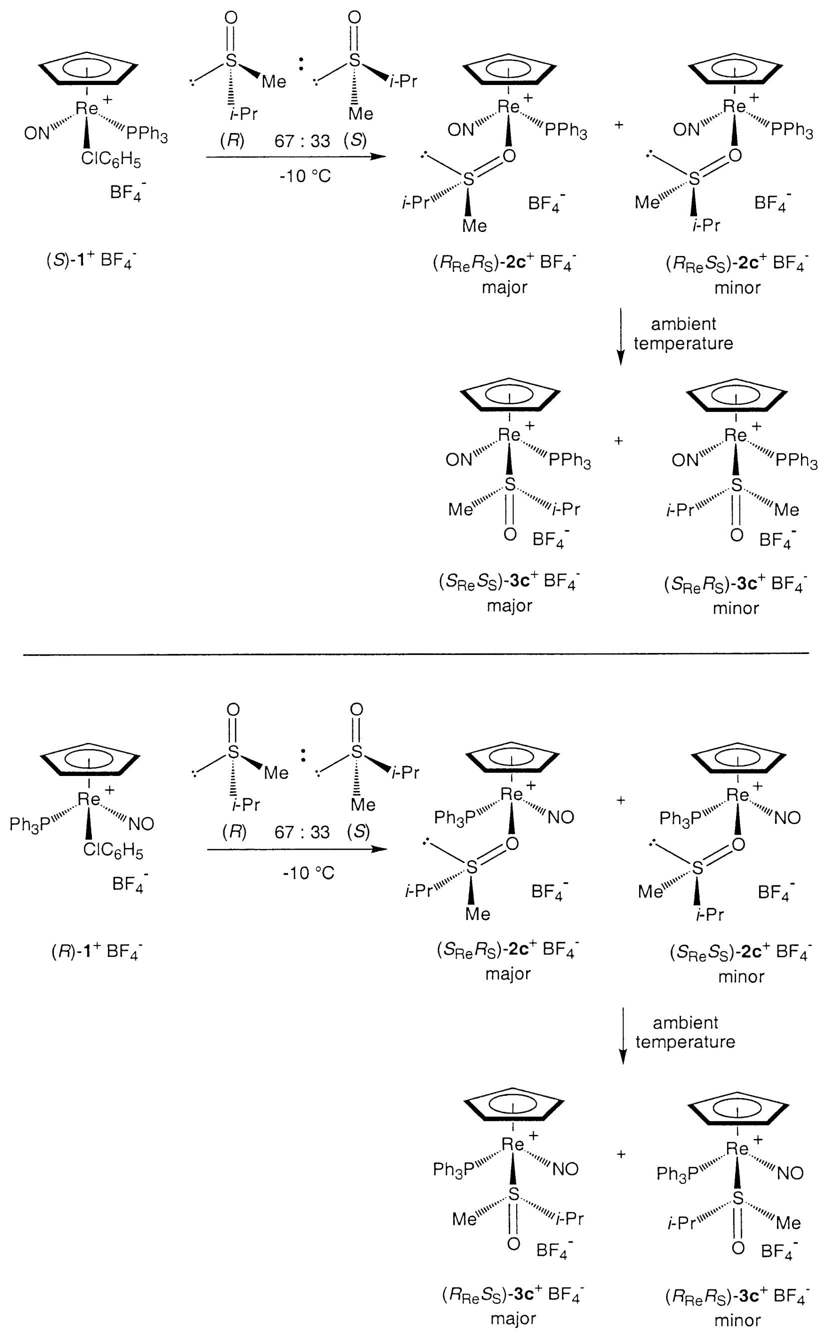

Scheme 2 Representative configurational assignments.

from reactions of non-racemic $\mathbf{1}^+BF_4^-$ and sulfoxide **d**, and (3) the literature configuration of non-racemic **d** (which has sometimes been a point of confusion).[21]

3 Reactions of sulfoxide complexes

Various reactions were conducted with the hope of clarifying aspects of the preceding data. First, the oxygen-bound DMSO complex $\mathbf{2a}^+BF_4^-$ was dissolved in DMSO-d_6 and the sample monitored by ^{1}H NMR. Rapid ligand exchange to give $\mathbf{2a}^+$-d_6 BF_4^- took place, followed by a slower linkage isomerism to $\mathbf{3a}^+$-d_6 BF_4^- (evident from the cyclopentadienyl resonances). Thus, oxygen-bound sulfoxide ligands undergo facile exchange. From previous studies of $[(\eta^5\text{-}C_5H_5)Re(NO)(PPh_3)(L)]^+$ systems an associative mechanism would be expected.[22] Only a twofold excess of sulfoxide ligand is used under the preparative conditions in Scheme 1, but such exchange constitutes a possible mechanism of sulfur epimerization and thereby diastereomer interconversion.

To further probe this point, a chlorobenzene solution of the oxygen-bound *t*-butyl methyl sulfoxide complex $\mathbf{2d}^+BF_4^-$ (non-racemic; 55 : 45 $S_{Re}R_S/S_{Re}S_S$) was treated with three equivalents of DMSO at room temperature. The reaction was monitored by ^{31}P NMR. As shown in eqn. (1), the oxygen-bound DMSO

(1)

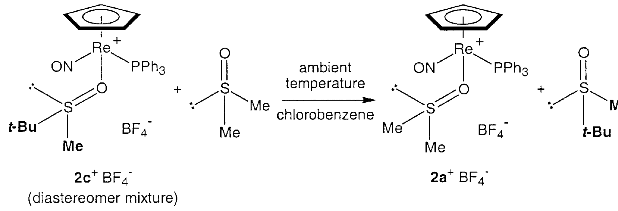

complex $\mathbf{2a}^+BF_4^-$ formed. After 1 h (*ca.* 60% conversion) some $\mathbf{3a}^+BF_4^-$ could be detected, and residual $\mathbf{2d}^+BF_4^-$ continued to react. Thus, degenerate ligand exchange should take place under the preparative conditions in Scheme 1.

A Pyrex NMR tube was charged with an acetone-d_6 solution of complex $\mathbf{3a}^+BF_4^-$ and an internal standard (Ph_3SiMe),

Table 2 Selected bond lengths (Å), bond angles (deg), and torsion angles (deg) in complex $(R_{Re}S_S,S_{Re}R_S)$-**2d**$^+$TfO$^-$·0.5CH$_2$Cl$_2$

Re–P	2.383(2)	Re–C1	2.23(1)
Re–O2	2.129(6)	Re–C2	2.28(1)
Re–N	1.781(8)	Re–C3	2.33(1)
S1–O2	1.549(6)	Re–C4	2.31(1)
N–O1	1.16(1)	Re–C5	2.23(1)
P–C6	1.826(9)	S1–C24	1.79(1)
P–C12	1.826(9)	S1–C25	1.84(1)
P–C18	1.814(9)		
O2–Re–P	81.2(2)	Re–N–O1	172.7(9)
O2–Re–N	103.3(4)	C1–C2–C3	108(1)
P–Re–N	91.0(3)	C2–C3–C4	110(1)
Re–O2–S1	115.0(4)	C3–C4–C5	107(1)
O2–S1–C24	103.1(5)	C4–C5–C1	107(1)
O2–S1–C25	101.3(5)	C5–C1–C2	108(1)
C24–S1–C25	103.0(6)		
C24–S1–O2–Re	86.4(5)	P–Re–O2–S1	−157.2(3)
C25–S1–O2–Re	−167.2(5)	N–Re–O2–S1	−68.2(4)
LP[a]–S1–O2–Re	−40.2(4)		

[a] LP = Lone pair.

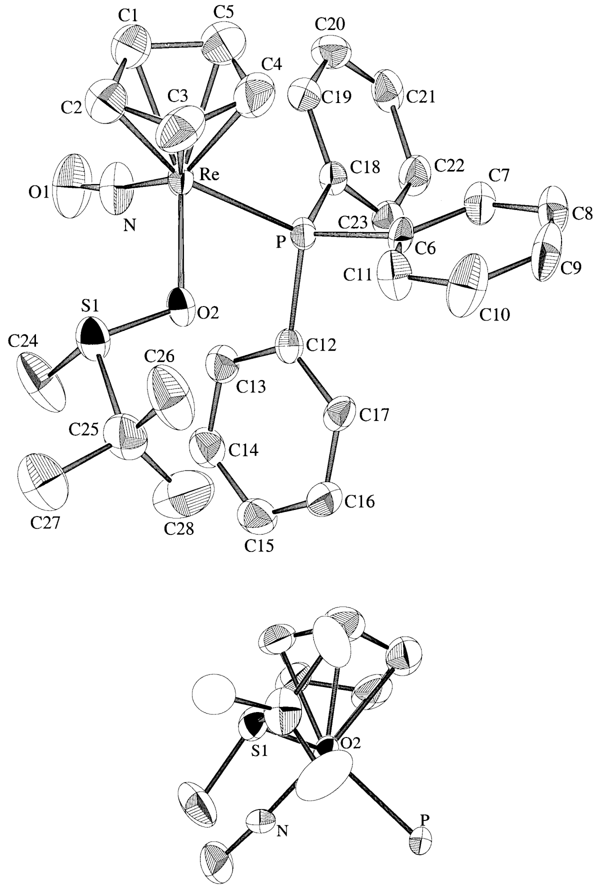

Fig. 1 Structure of the cation of the *t*-butyl methyl sulfoxide complex $(R_{Re}S_S,S_{Re}R_S)$-[(η^5-C$_5$H$_5$)Re(NO)(PPh$_3$)(O=S(Me)*t*-Bu)]$^+$TfO$^-$·0.5 CH$_2$Cl$_2$ ($(R_{Re}S_S,S_{Re}R_S)$-**2d**$^+$TfO$^-$·0.5CH$_2$Cl$_2$): Top, numbering diagram. Bottom, Newman-type projection with phenyl rings omitted.

and photolysed at −70 °C using a Hannovia 450 W mercury lamp. After 10 min, **3a**$^+$BF$_4$$^-$, linkage isomer **2a**$^+BF_4$$^-$, and the previously characterized[23] acetone-d_6 complex [(η^5-C$_5$H$_5$)Re(NO)(PPh$_3$)(η^1-O=C(CD$_3$)$_2$)]$^+$BF$_4$$^-$ had formed in 83, 13, and 4% yields, as determined by ^{1}H and ^{31}P NMR. A second photolysis was conducted for 13 minutes at ambient temperature. This gave **3a**$^+$BF$_4$$^-$, **2a**$^+BF_4$$^-$, the acetone complex, and various unidentified species in 35, 36, 15, and 14% yields. Subsequent thermal (dark) reactions then occurred. First the acetone complex converted into **2a**$^+$BF$_4$$^-$. Then this isomerized to **3a**$^+$BF$_4$$^-$. Other photoinduced and contrathermodynamic linkage isomerizations of sulfur-bound DMSO complexes have recently been reported.[24]

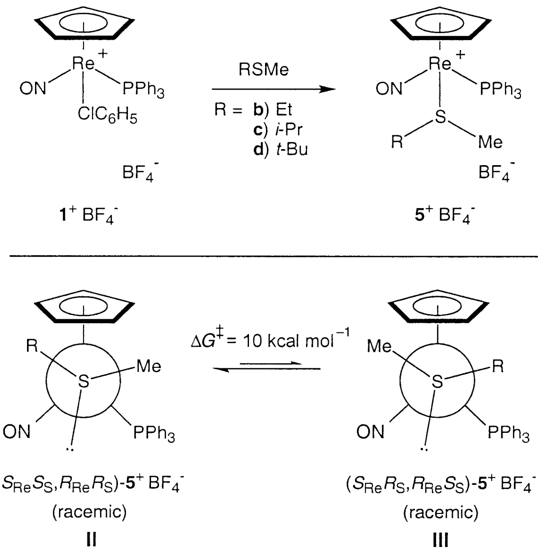

Scheme 3 Representative syntheses of sulfide complexes and configurational equilibria.

4 Syntheses and oxidations of sulfide complexes

As noted in the Introduction, the major impetus for the above syntheses and structural assignments was to provide a solid foundation for analysing oxidations of the corresponding sulfide complexes, [(η^5-C$_5$H$_5$)Re(NO)(PPh$_3$)(S(Me)R)]$^+$X$^-$ (**5a**–**5d**$^+$X$^-$). The triflate salts **5a**–**5d**$^+$TfO$^-$ were synthesized from the free sulfides and triflate complex **4** earlier, and the tetrafluoroborate salt **5a**$^+$BF$_4$$^-$ was prepared *via* a dichloromethane complex.[7] The new tetrafluoroborate salts **5b**–**5d**$^+$BF$_4$$^-$ were similarly prepared from the chlorobenzene complex **1**$^+$BF$_4$$^-$, as shown in Scheme 3. Their ^{1}H and ^{31}P NMR spectra were essentially identical to those of the triflates.[7] Note that **5b**–**5d**$^+$X$^-$ have both rhenium and sulfur stereocenters. Variable temperature NMR experiments with **5a**$^+$TfO$^-$ and a di(methallyl) sulfide complex established low sulfur inversion/rotation barriers (9.4–9.8 kcal mol^{-1}).[7,9a] Low temperature NMR spectra of the unsymmetrical sulfide complexes **5b**, **5c**$^+$TfO$^-$ showed decoalesence to two diastereomers (67 : 33 and 77 : 23). The major and minor have been assigned $S_{Re}S_S$, $R_{Re}R_S$ and $S_{Re}R_S$,$R_{Re}S_S$ configurations, respectively, as illustrated by **II** and **III** in Scheme 3.[7]

Screening experiments were conducted with complex **5a**$^+$TfO$^-$ and several oxidizing agents. No reactions were observed with pyridine *N*-oxide, trimethylamine *N*-oxide, and the peracid MCPBA (*m*-chloroperbenzoic acid). Hydrogen peroxide gave some DMSO complex **3a**$^+$TfO$^-$, but dimethyldioxirane[25] was more promising. This reagent had previously been employed to oxidize ligands in organometallic complexes.[26] Accordingly, NMR tubes were charged with **5a**–**5d**$^+$X$^-$ and cooled to −80 °C. Standardized acetone solutions of dimethyldioxirane (3 equivalents) were added. The tubes were transferred to 0 °C NMR probes and ^{31}P spectra periodically recorded. The bulkier sulfide complexes (and to a lesser extent the triflate salts) reacted more slowly. Only in the case of **5d**$^+$X$^-$ did a substantial amount of educt remain after 3 h. As summarized in Scheme 4, sulfoxide complexes **3a**–**3d**$^+$X$^-$ formed in fair to good yields, and **3b**–**3d**$^+$X$^-$ with fair to good diastereoselectivity. The major diastereomer always corresponded to that which would be obtained by oxygen atom transfer to the lone pair in **II** (Scheme 3). However, variable amounts of the phosphine oxide Ph$_3$P=O were also generated.

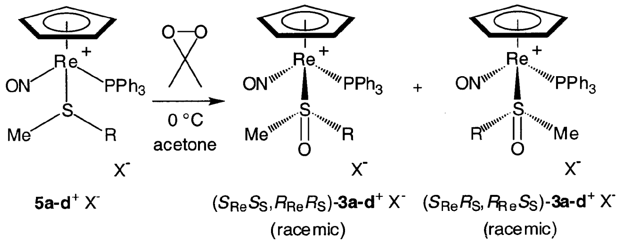

Educt	Product ratio (%)			Conversion (time)^a
	($S_{Re}S_S$,$R_{Re}R_S$)-**3**$^+$ (major)	($S_{Re}R_S$,$R_{Re}S_S$)-**3**$^+$ (minor)	$Ph_3P{=}O$	
5a$^+$ BF_4^-	67		33	96 (2.3 h)
5b$^+$ BF_4^-	49	24	27	100 (2.0 h)
5b$^+$ TfO^-	53	21	25	91 (2.6 h)
5c$^+$ BF_4^-	84	10	6	97 (3.6 h)
5c$^+$ TfO^-	84	11	5	85 (3.0 h)
5d$^+$ BF_4^-	100	-^{b}	-^{b}	39 (3.0 h)
5d$^+$ TfO^-	77	-^{b}	23	38 (5.6 h)
5d$^+$ TfO^-	58	-^{b}	42	79 (2 d)^c
5d$^+$ TfO^-	32	-^{b}	68	100 (4 d)^d

^{a}0 °C in acetone. ^{b}Not observed. ^{c}-20 °C. ^{d}Ambient temperature.

Scheme 4 Oxidation of sulfide complexes.

Efforts were made to minimize and/or better understand the origin of the phosphine oxide. After the educts **5a**–**5d**$^+X^-$ were consumed the product ratios did not appear to change with time. Reactions at higher temperatures gave greater proportions of phosphine oxide. Only in rare instances has PPh_3 been observed to dissociate from adducts of the chiral rhenium Lewis acid **I**.[27] In these cases it can be replaced by the more basic phosphine P(*p*-$MeC_6H_4)_3$.[27] Accordingly, the sulfide complex **5b**$^+TfO^-$ and the DMSO complex **3a**$^+TfO^-$ were combined with an excess of P(*p*-$MeC_6H_4)_3$ (15–20 equivalents) in acetone. No reactions were observed after several hours at 50 °C. Finally, **3a**$^+BF_4^-$ and dimethyldioxirane (3.0 equivalents) were combined in acetone at −80 °C. The sample was monitored by ^{31}P NMR at 0 °C. Phosphine oxide formed at a rate similar to that in the oxidation of **5a**$^+BF_4^-$. Thus, a competitive overoxidation seems at present the best explanation for phosphine oxide formation. No effort was made to identify the corresponding rhenium-containing product. Note that it might rapidly consume additional oxidizing equivalents.

Discussion

1 Sulfoxide ligand binding selectivities

The data in Scheme 1 show that, regardless of the rhenium electrophile employed, the sterically more accessible sulfoxide oxygen is the kinetically preferred binding site. This trend has precedent, but is seldom rigorously established from preparative experiments alone. For example, a platinum complex containing both oxygen- and sulfur-bound DMSO has been carefully studied.[28] NMR data show that the oxygen-bound ligand exchanges much faster with free DMSO, and exclude initial sulfur binding. Also, numerous complexes with both oxygen- and sulfur-bound sulfoxide ligands have been structurally characterized.[29] The "cone angles" and other steric properties of the two binding modes have been quantitatively compared,[18b,30] and by every criterion the oxygen-bound form is less bulky.

In contrast to the linkage isomer ratios, the diastereomer ratios of **2b**–**2d**$^+X^-$ cannot be so easily interpreted. Variables include the precipitative work-ups (which can favor the less soluble diastereomer), the degree of isomerization to **3b**–**3d**$^+X^-$ (one diastereomer can react faster), and the facile exchange of the oxygen-bound sulfoxide ligands with free sulfoxides (an epimerization mechanism; eqn. (1)), all of which are condition-dependent and probably contribute to the modest reproducibilities (Scheme 1). The large difference between **2d**$^+BF_4^-$ and **2d**$^+TfO^-$ (and **2c**$^+BF_4^-$ and **2c**$^+TfO^-$) makes it very improbable that ratios are under thermodynamic control. There also might be a dependency upon the precursors, chlorobenzene complex **1**$^+BF_4^-$ and triflate complex **4**. Based upon limited data (*e.g.*, its slow racemization in benzene),[17] substitution reactions of **4** are believed to proceed differently from other functional equivalents of rhenium Lewis acid **I**.

Within detection limits (≈1%), complexes **2a**–**2c**$^+X^-$ completely isomerize to **3a**–**3c**$^+X^-$ in solution. Hence, the thermodynamic binding affinities of the sulfoxide ligand sulfur atoms are at least two orders of magnitude greater. Owing to the poor mass balance, the direction of the equilibrium for the bulkier S-*t*-Bu complexes **2d**$^+X^-$/**3d**$^+X^-$ is less obvious. However, since no oxygen-bound isomer is detected under the conditions of Scheme 4 (note some oxidations of **5d**$^+TfO^-$ are executed at room temperature), the sulfur-bound isomer is likely more stable. Each linkage isomerization is further characterized by a kinetic and thermodynamic diastereoselectivity. We analyse the latter below, in conjunction with the oxidations. Since the diastereomer ratios for **3b**,**3c**$^+X^-$ are so close to 50 : 50 (Scheme 1), they likely (in view of other data given below) represent kinetic ratios.

It is worth emphasizing that the isomerizations in Scheme 1 are conducted in the presence of an excess of sulfoxide. Coupled with the facile exchange of the oxygen-bound ligands with free sulfoxides, there is no requirement, under any mechanistic scenario, for the diastereomer ratios to match before and after isomerization. The isomerizations involving non-racemic educts (*e.g.* Scheme 2) are conducted with only slight excesses of sulfoxide (0–25%). Here, close correspondences are observed. Linkage isomerization could occur by at least three mechanisms: (1) an intramolecular 1,2 migration of rhenium; (2) a dissociation/recoordination process; (3) an associative substitution when free sulfoxide is present. We have shown that η^2/η^1 isomerizations of aldehyde complexes of **I** proceed *via* intramolecular mechanisms,[31] as well as higher energy processes involving migrations between carbonyl donors and alkenes.[32,33] Hence, we currently favor the first possibility.

Returning to the thermodynamics of linkage isomerization, there are many metal fragments that preferentially give sulfur-bound sulfoxide complexes, and many others that give oxygen-bound sulfoxide complexes.[18] Literature analyses are often cast in terms of hard/soft acid/base theory. We prefer to focus upon steric and electronic properties. The rhenium Lewis acid **I** is quite bulky, but not so congested that the sulfur-bound isomers become less stable. **I** is furthermore a strong π donor, and from an electronic standpoint matches better with the stronger π acceptor, the sulfur-bound sulfoxide. Linkage isomerizations that dramatically illustrate the importance of such electronic factors are shown in Scheme 5. The ruthenium Lewis acid

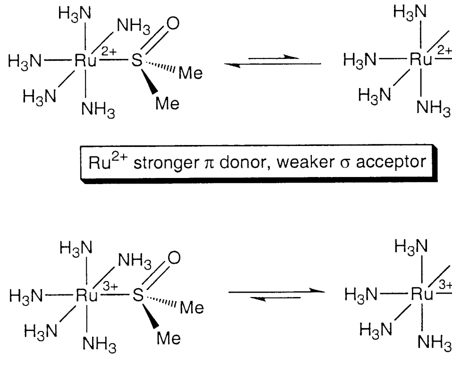

Scheme 5 Electronic effects in sulfoxide ligand linkage isomerization.

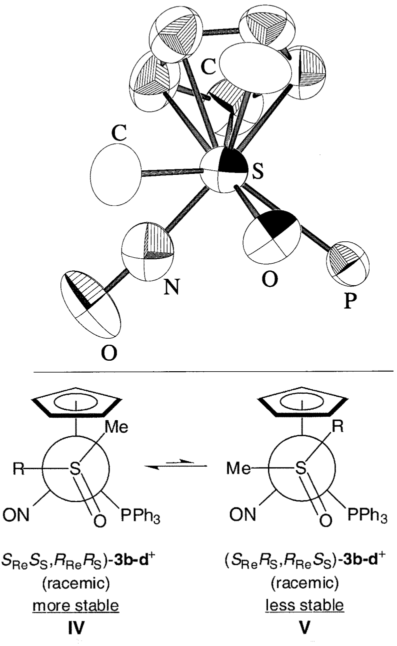

Fig. 2 Top: structure of the cation of sulfur-bound DMSO complex **3a**$^+$BF$_4^-$ with phenyl rings omitted. Bottom: possible direction of diastereomeric equilibrium for **3b**–**3d**$^+$BF$_4^-$.

[(H$_3$N)$_5$Ru]$^{2+}$ strongly favors sulfur-bound isomers, but a one electron oxidation gives the weaker π donor and stronger σ acceptor [(H$_3$N)$_5$Ru]$^{3+}$, which strongly favors oxygen-bound isomers.[16a–e]

2 Structural properties of sulfoxide complexes

The crystal structure of the oxygen-bound *t*-butyl methyl sulfoxide complex ($R_{Re}S_S,S_{Re}R_S$)-**2d**$^+$TfO$^-$ (Fig. 1) can be compared to that of the sulfur-bound DMSO complex **3a**$^+$BF$_4^-$ reported earlier.[7] A partial view of the latter is given in Fig. 2. To our knowledge, these are the only structurally characterized oxygen- and sulfur-bound *mono*sulfoxide complexes of the same metal fragment in the literature. Many crystal structures of complexes with both oxygen- and sulfur-bound sulfoxide ligands have been determined,[29,30] but the ligands always possess electronically and sterically distinct coordination environments.[34]

As observed for all adducts of the Lewis acid **I**, complex ($R_{Re}S_S,S_{Re}R_S$)-**2d**$^+$TfO$^-$ exhibits a formally octahedral geometry at rhenium. However, the angles between the η^1 ligands (81.2(2), 103.3(4), 91.0(3)°) deviate somewhat more from 90° than usual, especially in comparison to **3a**$^+$BF$_4^-$ and similar dialkyl sulfide complexes.[7,9a] The rhenium–oxygen bond (2.129(6) Å) is shorter than the rhenium–sulfur bond in **3a**$^+$BF$_4^-$ (2.395(3) Å), while the sulfur–oxygen bond (1.549(6) Å) is longer than those in **3a**$^+$BF$_4^-$ (1.462(4) Å) and free DMSO (1.513(5) Å).[18b] These trends have abundant precedent in structures of other sulfoxide complexes.[18,29,34] Analogous distortions from octahedral geometries and X=O bond lengthenings occur upon σ coordination of ketones and aromatic aldehydes to **I**.[23,35]

As illustrated by the bottom view in Fig. 1, complex ($R_{Re}S_S,S_{Re}R_S$)-**2d**$^+$TfO$^-$ adopts a rhenium–oxygen conformation that directs the sulfur nearly *anti* to the bulky PPh$_3$ ligand. This is reflected by the P–Re–O–S torsion angle (−157.2(3)°). Similar conformations are found in other adducts of **I** and ligands with X–YABC groupings, such as alkoxides[27a] and alkyl halides.[36] Many experiments have shown that the interstice between the cyclopentadienyl and nitrosyl ligands is the least congested. Complex ($R_{Re}S_S,S_{Re}R_S$)-**2d**$^+$TfO$^-$ also adopts an oxygen–sulfur conformation that places the large *t*-butyl substituent nearly *anti* to the bulky rhenium, as indicated by the Re–O–S–C25 torsion angle (167.2(5)°). Analogous features are observed in the crystal structures of other adducts of **I** and X–YABC ligands.[8,27a,36,37]

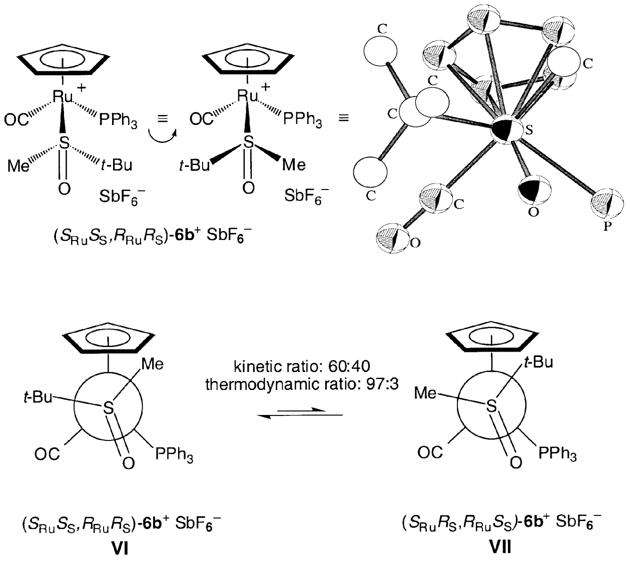

Fig. 3 Structures and diastereomeric equilibria for a ruthenium sulfur bound *t*-butyl methyl sulfoxide complex. Phenyl rings are omitted from the ORTEP.

As noted earlier, complex **3a**$^+$BF$_4^-$ adopts an unusual rhenium–sulfur conformation in which the oxygen and bulky PPh$_3$ ligand are nearly *syn*.[7] This is reflected by the P–Re–S–O torsion angle (−17.2(3)°). Normally the smallest group on the ligating atom would give a −60 to −70° torsion angle, as illustrated by the sulfur lone pair positions in the sulfide complexes **II** and **III** (Scheme 3). The contrasteric rhenium–sulfur conformation is one of two that would maximize back bonding from the d orbital HOMO of **I** to the S=O acceptor orbital.[7] This is in accord with the much higher IR ν_{NO} values of the sulfur-bound complexes **3**$^+$X$^-$.

Faller and Ma has reported the crystal structure of the sulfur-bound ruthenium *t*-butyl methyl sulfoxide complex ($S_{Ru}S_S,R_{Ru}R_S$)-[(η^5-C$_5$H$_5$)Ru(CO)(PPh$_3$)(S(=O)(Me)*t*-Bu)]$^+$-SbF$_6^-$ (($S_{Ru}S_S,R_{Ru}R_S$)-**6d**$^+$SbF$_6^-$).[6a] A partial view is given in Fig. 3. The ruthenium fragment is essentially isoelectronic and isostructural with our rhenium fragment. The sulfoxide is identical to that in ($R_{Re}S_S,S_{Re}R_S$)-**2d**$^+$TfO$^-$, while the bonding mode is analogous to that of the DMSO in **3a**$^+$BF$_4^-$. The metal–sulfur conformation is similar to that of **3a**$^+$BF$_4^-$ (P–M–S–O torsion angle −28.3°). Other important observations of Faller and Ma are described in the following section.

3 Configurational equilbria

The above structural data provide starting points for models that predict the relative stabilities of the diastereomers of **2b**–**2d**$^+$X$^-$ and **3b**–**3d**$^+$X$^-$. Although this represents a digression from what we could verify experimentally, we believe the analysis belongs in the literature as an aid to future research. First, we have reported the crystal structure of the alkoxide complex ($R_{Re}S_C,S_{Re}R_C$)-(η^5-C$_5$H$_5$)Re(NO)(PPh$_3$)(OCH(Me)Ph) (($R_{Re}S_C,S_{Re}R_C$)-**7**), an adduct of Lewis acid **I** and a ligand of the type X–YABC.[27a] The atom β to rhenium (Y) has groups (A, B, C) similar in relative sizes to those in ($R_{Re}S_S,S_{Re}R_S$)-**2b**–**2d**$^+$X$^-$. As shown by **VIII** in Scheme 6, the alkoxide adopts a similar conformation in the solid state, with approximately *anti* P–Re–O–C and Re–O–C–Ph linkages.

Furthermore, the diastereomers of complex **7** equilibrate by a mechanistically well defined PPh$_3$ dissociation/β-hydride elimination process.[27a] Complex ($R_{Re}R_C,S_{Re}S_C$)-**7**, shown in **IX** with the same *anti* conformations found in crystalline ($R_{Re}S_C$,-$S_{Re}R_C$)-**7**, proved to be less stable. This was ascribed to inter-

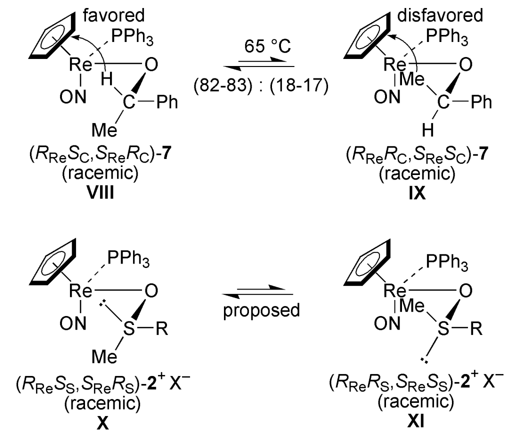

Scheme 6 Relative stabilities of diastereomeric alkoxide and oxygen-bound sulfoxide complexes of the rhenium Lewis acid **I**.

actions between the medium-sized cyclopentadienyl rhenium ligand and the alkoxide methyl substituent. Although both diastereomers would adopt an ensemble of conformations in solution, this model successfully correlated all data, including stability trends of related amido complexes.[27b]

The similar crystal structure of the oxygen-bound sulfoxide complex $(R_{Re}S_S,S_{Re}R_S)$-**2d**$^+$TfO$^-$ suggests that it should be possible to extend this model to $(R_{Re}S_S,S_{Re}R_S)$-**2b**–**2d**$^+$X$^-$ and $(R_{Re}R_S,S_{Re}S_S)$-**2b**–**2d**$^+$X$^-$. As illustrated by **X** and **XI** in Scheme 6, the former should be more stable. Accordingly, with the bulkier sulfoxides **c** and **d** the $R_{Re}S_S,S_{Re}R_S$ diastereomer (**X**) dominates under the conditions of Scheme 1. Under the conditions of Scheme 2 the opposite diastereomer of **2c**$^+$BF$_4^-$, $(R_{Re}R_S)$-**2c**$^+$BF$_4^-$ or the enantiomer $(S_{Re}S_S)$-**2c**$^+$BF$_4^-$ appears to isomerize slightly faster, consistent with a lower stability.

With respect to the relative diastereomer stabilities of the sulfur-bound complexes **3b**–**3d**$^+$X$^-$, consider first structures **IV** and **V** in Fig. 2. Based upon data with equilibratible diastereomeric alkyl complexes of the type $(\eta^5$-$C_5H_5)$Re(NO)(PPh$_3$)(CHRR′),[38] **IV** should be the more stable. However, closer precedent is available from the Faller and Ma study. They monitored the generation of **6d**$^+$SbF$_6^-$ (Fig. 3) from an acetone complex by NMR. No oxygen-bound sulfoxide complex was detected, and a 60 : 40 $S_{Ru}S_S,R_{Ru}R_S/S_{Ru}R_S,R_{Ru}S_S$ kinetic mixture formed. This system is configurationally labile at ruthenium, and equilibrated to a 97 : 3 $S_{Ru}S_S,R_{Ru}R_S/S_{Ru}R_S$, $R_{Ru}S_S$ mixture in dichloromethane at room temperature. Care was taken to ensure that the major component was crystallographically characterized. Hence, analogous stability trends can confidently be predicted for **3b**–**3d**$^+$X$^-$.

These assignments allow another issue to be addressed. Would the mechanism of isomerization of complexes **2b**–**2d**$^+$X$^-$ to **3b**–**3d**$^+$X$^-$ favored above, intramolecular 1,2-migration, with retention at rhenium and sulfur, correlate a more stable diastereomer with a more stable diastereomer, or a more stable diastereomer with a less stable diastereomer? As can be visualized from the bottom structure in Fig. 1 or **X** in Scheme 6, $(R_{Re}S_S,S_{Re}R_S)$-**2d**$^+$TfO$^-$, the more stable diastereomer by the model in Scheme 6, would give the less stable diastereomer of the linkage isomer $(S_{Re}R_S,R_{Re}S_S)$-**3d**$^+$TfO$^-$.[14b] This might account for the lower isomerization yields with *t*-butyl methyl sulfoxide.

4 Oxidation chemistry

Dimethyldioxirane often gives much cleaner reactions than other oxygen atom transfer reagents.[25] However, except at low conversions, reactions with sulfide complexes **3a**–**3d**$^+$X$^-$ give significant amounts of phosphine oxide by-product (Scheme 4). Our data give no special insight into the origin of this material, except for excluding phosphine dissociation. It appears to form by a competitive overoxidation, possibly involving oxygen atom transfer to rhenium or the sulfoxide ligand oxygen.[39] Some type of internal elimination would then lead to phosphine oxide.

In closely related work, Schenk *et al.* used dimethyldioxirane to oxidize a variety of sulfide complexes of bis(phosphine) ruthenium Lewis acids $[(\eta^5$-$C_5H_5)$Ru(PR$_2$R′)$_2]^+$ to the corresponding sulfoxide complexes.[5a,b] Fourfold excesses were generally employed, and yields were with only a few exceptions very high. However, when adducts of the less electron rich carbonyl monophosphine Lewis acid $[(\eta^5$-$C_5H_5)$Ru(CO)(PPh$_3$)$]^+$ were employed (giving homologs of the Faller complex $(S_{Ru}S_S$, $R_{Ru}R_S)$-**6d**$^+$SbF$_6^-$ above), yields were much lower.[5b] For example, the isopropyl methyl sulfoxide complex $[(\eta^5$-$C_5H_5)$Ru(CO)(PPh$_3$)(S(=O)(Me)*i*-Pr)$]^+$PF$_6^-$ (**6c**$^+$PF$_6^-$) was obtained in 45% yield and as a 64 : 36 ratio of diastereomers. Large excesses of dimethyldioxirane did not lead to improvements.

Since oxidations of both Schenk's ruthenium carbonyl and our rhenium nitrosyl systems are plagued by side-reactions the relative diastereoselectivities become less meaningful. A few comparisons are made in the ESI. Some of Schenk's best data are summarized in Scheme 7.[5a,b] The commercially available chiral diphosphine chiraphos, (2*S*,3*S*)-2,3-bis(diphenylphosphino)butane, enables the highly diastereoselective oxidation of a number of sulfide ligands. Subsequent reactions with iodide liberate non-racemic sulfoxides, and the chiral ruthenium fragment can be recycled. A number of supporting crystal structures and mechanistic experiments were executed, and advanced applications in organic synthesis developed.[5,40]

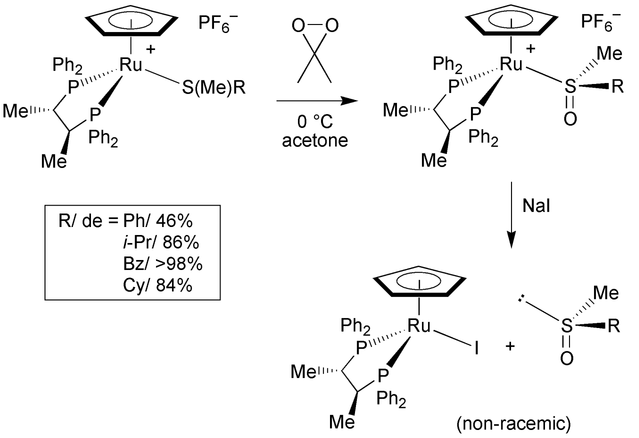

Scheme 7 Oxidation of chiral ruthenium sulfoxide complexes.

Conclusion

The coordination chemistry of sulfoxides has been extended by use of a chiral rhenium Lewis acid (**I**) that gives divergent kinetic and thermodynamic selectivities for oxygen- and sulfur-bound linkage isomers. This has enabled the first structural characterization of linkage isomers of identical metal fragments. The configurational stability of the rhenium Lewis acid is an advantage with respect to assigning the configurations of rhenium/sulfur diastereomers, but a disadvantage with respect to assigning relative diastereomer stabilities. Other literature data, including equilibrations of related ruthenium sulfoxide complexes, allow qualitative but not quantitative predictions. Dimethyldioxirane oxidations of the corresponding rhenium sulfide complexes also give sulfur-bound sulfoxide complexes. Several general attributes of transition metal sulfide and sulfoxide complexes give grounds for optimism that new enantioselective sulfide oxidation catalysts might be developed. However, for adducts of **I**, competing overoxidation of the sulfoxide complexes to Ph$_3$P=O is a problem. Diastereoselectivities are reasonable, but from every preparative standpoint a chiral bis(phosphine) ruthenium Lewis acid developed by Schenk is superior. Nonetheless, these data should be of immense use in the future design and development of new transition metal-based strategies for enantioselective oxidations of sulfides to sulfoxides.

Experimental

General methods

Most details are routine and fully described in the ESI.† Racemic and enantiomerically enriched sulfoxides O=S(Me)R were prepared by published methods.[4a,41] Dimethyldioxirane was generated in acetone by a literature procedure and standardized with PPh_3.[42] $HBF_4{\cdot}OEt_2$ (Aldrich) was standardized as previously described.[43]

Preparations

[(η^5-C_5H_5)Re(NO)(PPh_3)(O=S(Me)R)]$^+BF_4^-$ ($2^+BF_4^-$) (R = Me a, Et b, *i*-Pr c or *t*-Bu d). A Schlenk flask was charged with (η^5-C_5H_5)Re(NO)(PPh_3)(CH_3) **8**[44] (0.446 g, 0.798 mmol) and C_6H_5Cl (4 mL) and cooled to −45 °C (CH_3CN/CO_2). Then $HBF_4{\cdot}OEt_2$ (0.105 mL, 0.819 mmol) was added with stirring to generate [(η^5-C_5H_5)Re(NO)(PPh_3)(ClC_6H_5)]$^+BF_4^-$ (**1**$^+BF_4^-$).[12] After 10 min O=SMe_2 (0.127 g, 1.63 mmol) was added. After 15 min the −45 °C bath was replaced by a −15 °C bath (ethylene glycol/CO_2). After 1 h an orange precipitate began to form. After an additional 0.5 h diethyl ether was added. The precipitate was collected by filtration, washed with ether (2 × 10 mL), and dried *in vacuo* to give an orange powder that was a 90 : 10 **2a**$^+$/**3a**$^+BF_4^-$ mixture (0.475 g, 0.670 mmol, 84%).[45] IR: ν_{NO} 1685 vs, ν_{SO} 891 m cm^{-1}.[46] Complexes **2b**–**2d**$^+BF_4^-$ were prepared by analogous procedures as detailed in the ESI.[45] IR: ν_{NO} 1668/1670/1670 vs, ν_{SO} 888/889/886 m.[46] NMR: Table 1.

[(η^5-C_5H_5)Re(NO)(PPh_3)(O=S(Me)R)]$^+$TfO$^-$ (2^+TfO$^-$) (R = *i*-Pr c or *t*-Bu d). A Schlenk flask was charged with (η^5-C_5H_5)Re(NO)(PPh_3)(OTf) **4**[17] (0.471 g, 0.680 mmol), C_6H_5Cl (6 mL), O=S(Me)*i*-Pr (0.116 g, 1.10 mmol), and a stir bar. The sample was stirred for 5 h at 0 °C. The precipitate was collected by filtration, washed with C_6H_5Cl (3 × 5 mL) and ether (2 × 10 mL), and dried *in vacuo* to give an orange powder that was a 85 : 15 **2c**$^+$/**3c**$^+$TfO$^-$ mixture (0.345 g, 0.431 mmol, 63%).[45] IR: ν_{NO} 1674 vs, ν_{SO} 890 m cm^{-1}.[46,47] Complex **4** (0.523 g, 0.755 mmol), C_6H_5Cl (3 mL), and O=S(Me)*t*-Bu (0.117 g, 0.973 mmol) were combined in an analogous procedure. A similar work-up gave **2d**$^+$TfO$^-$ as an orange powder (0.512 g, 0.630 mmol, 83%), mp 104–106 °C (decomp.).[45] IR: ν_{NO} 1671 vs, ν_{SO} 885 s cm^{-1}.[46,47]

[(η^5-C_5H_5)Re(NO)(PPh_3)(S(=O)(Me)R)]$^+BF_4^-$ ($3^+BF_4^-$) (R = Et b, *i*-Pr c or *t*-Bu d). A Schlenk flask was charged with complex **8** (0.377 g, 0.675 mmol) and C_6H_5Cl (3 mL) and cooled to −45 °C. Then $HBF_4{\cdot}OEt_2$ (0.0870 mL, 0.679 mmol) was added with stirring to generate **1**$^+BF_4^-$. After 10 min, O=S(Me)Et (0.0790 g, 0.879 mmol) was added. After 15 min the cold bath was removed. After 1 h a red-orange precipitate began to form, which slowly became yellow. After an additional 11 h ether was added. The precipitate was collected by filtration, washed with ether (2 × 10 mL), and dried *in vacuo* to give **3b**$^+BF_4^-$ as a yellow powder (0.452 g, 0.625 mmol, 93%), mp 123–124 °C (decomp.)[45] Calc. for $C_{26}H_{28}BF_4NO_2PReS$: C, 43.22; H, 3.91. Found: C, 43.25; H, 3.92%. IR: ν_{NO} 1722 vs cm^{-1}.[46] Complexes **3c**,**3d**$^+BF_4^-$ were prepared by analogous procedures as detailed in the ESI. **3c**$^+BF_4^-$: mp 94–97 °C (decomp.).[45] Calc. for $C_{27}H_{30}BF_4NO_2PReS$: C, 44.03; H, 4.11. Found: C, 44.29; H, 4.09%. IR: ν_{NO} 1717 vs cm^{-1}.[46] **3d**$^+BF_4^-$: mp 152–153 °C (decomp.).[45] Calc. for $C_{28}H_{32}BF_4NO_2PReS$: C, 44.80; H, 4.30. Found: C, 44.62; H, 4.28%. IR: ν_{NO} 1720 vs cm^{-1}.[46] NMR: Table 1.

[(η^5-C_5H_5)Re(NO)(PPh_3)(S(=O)(Me)R)]$^+$TfO$^-$ (3^+TfO$^-$) (R = Et b or *i*-Pr c). Complex **4** (0.634 g, 0.916 mmol), C_6H_5Cl (5 mL), and O=S(Me)Et (0.173 g, 1.878 mmol) were combined in a procedure analogous to that given for **2c**$^+$TfO$^-$. The sample was stirred for 5 h at room temperature. A similar work-up gave **3b**$^+$TfO$^-$ as a yellow powder (0.670 g, 0.854 mmol, 93%), mp 116–117 °C (decomp.).[45] IR: ν_{NO} 1722 vs, ν_{SO} 1113 s cm^{-1}.[46,47] Complex **4** (0.531 g, 0.767 mmol), C_6H_5Cl (8 mL), and O=S(Me)*i*-Pr (0.147 g, 1.39 mmol) were combined in an analogous procedure. A similar work-up gave **3c**$^+$TfO$^-$ as a yellow powder (0.458 g, 0.573 mmol, 75%), mp 138–139 °C (decomp.).[45] IR: ν_{NO} 1716 vs, ν_{SO} 1119 s cm^{-1}.[46,47]

Non-racemic complexes. The following are representative, and additional experiments are detailed elsewhere (NMR shifts: see text).[20] **A.** A NMR tube was charged with complex (*S*)-**8** (0.0262 g, 0.0469 mmol)[44] and C_6H_5Cl (0.7 mL) and cooled to −45 °C. Then $HBF_4{\cdot}OEt_2$ (0.0063 mL, 0.049 mmol) was added to generate (*S*)-**1**$^+BF_4^-$.[12] After 10 min (*R*)-O=S(Me)*i*-Pr (0.0065 g, 0.061 mmol, 34% ee) was added. The tube was transferred to a −10 °C NMR probe and ^{31}P NMR spectra were recorded (20 min intervals, 5 h). The tube was kept at −20 °C overnight, giving **2c**$^+BF_4^-$ as a 68 : 32 $R_{Re}R_S/S_{Re}S_S$ mixture (93% conversion). The tube was transferred to a 25 °C NMR probe and ^{31}P NMR spectra were recorded (30 min intervals, 5 h). This gave **3c**$^+BF_4^-$ as a 78 : 22 $S_{Re}S_S/R_{Re}R_S$ mixture (83% isomerization). **B.** Complex (*R*)-**8** (0.0231 g, 0.0414 mmol), C_6H_5Cl (0.7 mL), $HBF_4{\cdot}OEt_2$ (0.0060 mL, 0.047 mmol) and (*R*)-O=S(Me)*i*-Pr (0.0047 g, 0.044 mmol, 34% ee) were combined as in experiment **A**. Then ^{31}P NMR spectra were recorded at −10 °C (20 min intervals, 5 h). After this time, **2c**$^+BF_4^-$ had formed as a 70 : 30 $S_{Re}R_S/S_{Re}S_S$ mixture (80% conversion). The probe was warmed to 25 °C and spectra were recorded (30 min intervals, 5 h). After this time, **3c**$^+BF_4^-$ was present as a 60 : 40 $R_{Re}S_S/R_{Re}R_S$ mixture (74% isomerization). **C.** Complex (*S*)-**8** (0.0207 g, 0.0371 mmol), C_6H_5Cl (0.7 mL), $HBF_4{\cdot}OEt_2$ (0.0050 mL, 0.039 mmol), and (*R*)-O=S(Me)*t*-Bu (0.0048 g, 0.040 mmol, 38% ee) were combined as in experiment **A**. Then ^{31}P NMR spectra were recorded at 20 min intervals for 5 h. **D.** Complex (*R*)-**8** (0.0219 g, 0.0392 mmol), C_6H_5Cl (0.7 mL), $HBF_4{\cdot}OEt_2$ (0.0055 mL, 0.043 mmol), and (*R*)-O=S(Me)*t*-Bu (0.0102 g, 0.0848 mmol, 38% ee) were combined and monitored as in experiment **C**.

Substitutions. The following is representative, and additional examples are detailed elsewhere.[20] A NMR tube was charged with complex **2a**$^+BF_4^-$ (0.0197 g, 0.0278 mmol) and DMSO-d_6 (0.6 mL, 0.66 g, 8.5 mmol) and transferred to a 22 °C NMR probe. Data: see text.

Photolyses. An E. J. Young NMR tube was charged with complex **3a**$^+BF_4^-$ (0.0070 g, 0.0099 mol), acetone-d_6 (0.7 mL), and Ph_3SiMe (0.0017 g, 0.0062 mmol). The tube was irradiated for 10 min at −70 °C with a 450 W Hannovia medium pressure mercury lamp. The tube was transferred to a −65 °C NMR probe and ^{31}P and ^1H NMR spectra were recorded. A second tube was charged with **3a**$^+BF_4^-$ (0.0064 g, 0.0090 mol), acetone-d_6 (0.6 mL), and Ph_3SiMe (0.0027 g, 0.0098 mmol), irradiated for 13 min at ambient temperature, and transferred to a 22 °C NMR probe. Data: see text.

[(η^5-C_5H_5)Re(NO)(PPh_3)(S(Me)R)]$^+BF_4^-$ ($5^+BF_4^-$) (R = Et b, *i*-Pr c or *t*-Bu d). A Schlenk flask was charged with complex **8** (0.352 g, 0.630 mmol) and C_6H_5Cl (3 mL) and cooled to −45 °C. Then HBF_4OEt_2 (0.0850 mL, 0.663 mmol) was added with stirring. After 10 min, S(Me)Et (0.144 g, 1.89 mmol) was added. After 15 min the cold bath was removed. After 2 h a yellow precipitate began to form. After 3 h more ether was added. The precipitate was collected by filtration, washed with ether (2 × 10 mL), and dried *in vacuo* to give **5b**$^+BF_4^-$ as a yellow powder (0.414 g, 0.585 mmol, 93%), mp 191–193 °C

Table 3 Summary of crystallographic data for $(R_{Re}S_S,S_{Re}R_S)$-$\mathbf{2d}^+TfO^-\cdot0.5CH_2Cl_2$

Chemical formula	$C_{29.5}H_{33}ClF_3NO_5PReS_2$
Formula weight	855.343
Crystal system	Triclinic
Space group	$P\bar{1}$ (no. 2)
a/Å	10.758(2)
b/Å	11.121(2)
c/Å	14.558(3)
α/°	102.47(2)
β/°	102.42(2)
γ/°	77.26(2)
V/Å^3	1632.79
Z	2
T/°C	−125
Reflections measured	5429
Total no. of unique data	5118
No. of observed data, $I > 3\sigma(I)$	4506
μ/cm^{-1}	40.80
R	0.043
R_w	0.053

(decomp.). Calc. for $C_{26}H_{28}BF_4NOPReS$: C, 44.20; H, 3.99. Found: C, 43.96; H, 3.91%. IR: ν_{NO} 1700 vs cm^{-1}.[46,47] Complexes **5c**,**5d**$^+BF_4^-$ were prepared by analogous procedures as detailed in the ESI. **5c**$^+BF_4^-$ (77%): mp 138–139 °C (decomp.). Calc. for $C_{27}H_{30}BF_4NOPReS$: C, 45.00; H, 4.20. Found: C, 45.27; H, 4.34%. IR: ν_{NO} 1700 vs cm^{-1}.[46,47] **5d**$^+BF_4^-$ (94%): mp 184–185 °C (decomp.). Calc. for $C_{28}H_{32}BF_4NOPReS$: C, 45.78; H, 4.39. Found: C, 45.65; H, 4.35%. IR: ν_{NO} 1700 vs cm^{-1}.[46,47]

Oxidations. A. The following is representative for sulfide complexes. A NMR tube was charged with complex **5c**$^+BF_4^-$ (0.0092 g, 0.012 mmol) and cooled to −80 °C. An acetone solution of dimethyldioxirane (0.80 mL, 0.037 mmol) was added. The tube was transferred to a 0 °C NMR probe, and ^{31}P NMR spectra were recorded (20 min intervals, 3 h). Data: Scheme 4. **B**. A NMR tube was charged with **3a**$^+TfO^-$ (0.0063 g, 0.0082 mmol) and acetone (0.3 mL) and cooled to −80 °C. An acetone solution of dimethyldioxirane (0.60 mL, 0.028 mmol) was added. The tube was transferred to a 0 °C NMR probe and ^{31}P NMR spectra were recorded (20 min intervals, 3 h).

Crystallography

An orange prism of complex $(R_{Re}S_S,S_{Re}R_S)$-$\mathbf{2d}^+TfO^-\cdot0.5\,CH_2Cl_2$ was obtained by vapor diffusion of hexane into a CH_2Cl_2 solution of $\mathbf{2d}^+TfO^-$. Data were collected as summarized in Table 3. Cell constants were obtained from 25 reflections with $15 < 2\theta < 25°$. The space group was determined from the lack of systematic absences and subsequent least-squares refinement. Lorentz, polarization, and empirical absorption (Ψ scans) corrections were applied. The structure was solved by standard heavy-atom techniques with the SDP/VAX package.[48] Non-hydrogen atoms were refined with anisotropic thermal parameters, except for the carbon, fluorine, and oxygen atoms of the triflate anion. The triflate exhibited static disorder and was refined isotropically with 1 : 1 occupancy. The CH_2Cl_2, located near the inversion center (edge), was also disordered. All non-CH_2Cl_2 hydrogen atom positions were calculated and added to the structure factor calculations. Scattering factors, and Δf and $\Delta f'$ values, were taken from the literature.[49]

CCDC reference number 151132.

See http://www.rsc.org/suppdata/dt/b0/b009533h/ for crystallographic data in CIF or other electronic format.

Acknowledgements

We thank the Deutsche Forschungsgemeinschaft (DFG; GL 300-1/4) and US National Science Foundation for support of this research.

References

1 A. Nudelman, *The Chemistry of Optically Active Sulfur Compounds*, Gordon and Breach, New York, 1984; A. J. Walker, *Tetrahedron*: *Asymmetry*, 1992, **3**, 961; M. C. Carreño, *Chem. Rev.*, 1995, **95**, 1717; M. Mikoajczk, J. Drabowicz and P. Kiebasiski, *Chiral Sulfur Reagents*, CRC Press, New York, 1997; A. Molina Ponce and L. E. Overman, *J. Am. Chem. Soc.*, 2000, **122**, 8672.

2 Reviews of catalytic methods: H. B. Kagan, in *Catalytic Asymmetric Synthesis*, ed. I. Ojima, VCH, New York, 1993, Ch. 4.3; C. Bolm, K. Muñiz and J. P. Hildebrand, in *Comprehensive Asymmetric Catalysis I-III*, eds. E. N. Jacobsen, A. Pfaltz and H. Yamamoto, Springer-Verlag, Berlin, 1999, Ch. 19.

3 Some catalytic methods reported subsequently to reference 2: M. A. M. Capozzi, C. Cardellicchio, G. Fracchiolla, F. Naso and P. Tortorella, *J. Am. Chem. Soc.*, 1999, **121**, 4708; M. Bonchio, G. Licini, F. Di Furia, S. Mantovani, G. Modena and W. A. Nugent, *J. Org. Chem.*, 1999, **64**, 1326; M. Bonchio, G. Licini, G. Modena, O. Bortolini, S. Moro and W. A. Nugent, *J. Am. Chem. Soc.*, 1999, **121**, 6258; S. Nimri and E. Keinan, *J. Am. Chem. Soc.*, 1999, **121**, 8978.

4 Representative full papers that describe stoichiometric methods: (*a*) P. Pitchen, E. Duñach, M. N. Deshmukh and H. B. Kagan, *J. Am. Chem. Soc.*, 1984, **106**, 8188; (*b*) F. A. Davis, R. T. Reddy, W. Han and P. J. Carroll, *J. Am. Chem. Soc.*, 1992, **114**, 1428; (*c*) D. A. Evans, M. M. Faul, L. Colombo, J. J. Bisaha, J. Clardy and D. Cherry, *J. Am. Chem. Soc.*, 1992, **114**, 5977.

5 Ruthenium-based methodology closely related to ours: (*a*) W. A. Schenk, J. Frisch, W. Adam and F. Prechtl, *Angew. Chem.*, *Int. Ed. Engl.*, 1994, **33**, 1609; W. A. Schenk, J. Frisch, W. Adam and F. Prechtl, *Angew. Chem.*, 1994, **106**, 1699; (*b*) W. A. Schenk, J. Frisch, M. Dürr, N. Burzlaff, D. Stalke, R. Fleischer, W. Adam, F. Prechtl and A. K. Smerz, *Inorg. Chem.*, 1997, **36**, 2372; (c) W. A. Schenk and M. Dürr, *Chem. Eur. J.*, 1997, **3**, 713; (*d*) W. A. Schenk, B. Steinmetz, M. Hagel, W. Adam and C. R. Saha-Möller, *Z. Naturforsch.*, *Teil B*, 1997, **52**, 1359.

6 Selected additional papers that feature chiral transition metal auxiliaries: (*a*) J. W. Faller and Y. Ma, *Organometallics*, 1992, **11**, 2726; (*b*) S. G. Davies and G. L. Gravatt, *J. Chem. Soc.*, *Chem. Commun.*, 1988, 780.

7 N. Quirós Méndez, A. M. Arif and J. A. Gladysz, *Organometallics*, 1991, **10**, 2199.

8 O. Meyer, A. M. Arif and J. A. Gladysz, *Organometallics*, 1995, **14**, 1844.

9 (*a*) P. C. Cagle, O. Meyer, K. Weickhardt, A. M. Arif and J. A. Gladysz, *J. Am. Chem. Soc.*, 1995, **117**, 11730; (*b*) P. C. Cagle, O. Meyer, D. Vichard, K. Weickhardt, A. M. Arif and J. A. Gladysz, *Organometallics*, 1996, **15**, 194; (*c*) Other relevant work by the authors: M. Otto, J. Parr and A. M. Slawin, *Organometallics*, 1998, **17**, 4527.

10 Data involving amido and phosphido complexes: (*a*) M. A. Dewey, D. A. Knight, A. M. Arif and J. A. Gladysz, *Chem. Ber.*, 1992, **125**, 815; (*b*) W. E. Buhro, B. D. Zwick, S. Georgiou, J. P. Hutchinson and J. A. Gladysz, *J. Am. Chem. Soc.*, 1988, **110**, 2427; (*c*) B. D. Zwick, M. A. Dewey, D. A. Knight, W. E. Buhro, A. M. Arif and J. A. Gladysz, *Organometallics*, 1992, **11**, 2673.

11 Schenk has also reported adducts of various sulfur donor ligands and **I**. For thiolate complexes and lead references to other species, see N. Burzlaff and W. A. Schenk, *Eur. J. Inorg. Chem.*, 1998, 2055.

12 J. J. Kowalczyk, S. K. Agbossou and J. A. Gladysz, *J. Organomet. Chem.*, 1990, **397**, 333.

13 All isomer ratios are normalized to 100, and error limits on each integer are ± 2; *e.g.* 58 : 42 ≡ (58 ± 2) : (42 ± 2).

14 (*a*) Rhenium configurations are given by a modified Cahn–Ingold–Prelog rule in which the cyclopentadienyl ligand is viewed as a pseudoatom of atomic number 30. This gives the priority sequence η^5-C_5H_5 > ClR > :S(=O)(Me)R > :S(Me)R > PPh_3 > :O=S(Me)R > NO > CH_3. See K. Stanley and M. C. Baird, *J. Am. Chem.*, *Soc.* 1975, **97**, 6598; T. E. Sloan, *Top. Stereochem.*, 1981, **12**, 1; C. Lecomte, Y. Dusausoy, J. Protas, J. Tirouflet and J. Dormand, *J. Organomet. Chem.*, 1974, **73**, 67. (*b*) The above priority sequence has confusing arbitrary consequences: (1) when the ClC_6H_5 ligand of $\mathbf{1}^+BF_4^-$ is replaced by :O=S(Me)R to give $\mathbf{2}^+BF_4^-$ with retention of *relative* configuration at rhenium, the *absolute* configuration of rhenium inverts; (2) when $\mathbf{2}^+X^-$ isomerizes to $\mathbf{3}^+X^-$ with retention of *relative* rhenium and sulfur configurations, the *absolute* configurations of rhenium *and* sulfur invert. (*d*) In line formulae, oxygen- and sulfur-bound sulfoxide ligands are specified as O=S(Me)R and S(=O)(Me)R, respectively.

15 W. E. Buhro, S. Georgiou, J. M. Fernández, A. T. Patton, C. E. Strouse and J. A. Gladysz, *Organometallics*, 1986, **5**, 956.

16 This trend is supported by many literature observations but is seldom explicitly discussed. References germane to an illustration in the discussion section: (a) A. Yeh, N. Scott and H. Taube, *Inorg. Chem.*, 1982, **21**, 2542; (*b*) M. Sano and H. Taube, *Inorg. Chem.*, 1994, **33**, 705; (*c*) A. Tomita and M. Sano, *Inorg. Chem.*, 1994, **33**, 5825; (*d*) B. J. Coe, T. J. Meyer and P. S. White, *Inorg. Chem.*, 1993, **32**, 4012; (*e*) J. J. Rack and H. B. Gray, *Inorg. Chem.*, 1999, **38**, 2.

17 J. H. Merrifield, J. M. Fernández, W. E. Buhro and J. A. Gladysz, *Inorg. Chem.*, 1984, **23**, 4022.

18 (*a*) J. A. Davies, *Adv. Inorg. Chem. Radiochem.*, 1981, **24**, 115; (*b*) M. Calligaris and O. Carugo, *Coord. Chem. Rev.*, 1996, **153**, 83.

19 (*a*) Some linkage isomerization occurs at 0 °C, and the normalized ratio of the δ 19.1, 18.9, 9.8, and 9.6 resonances is 56 : 26 : 11 : 7. (*b*) At this stage, the ratio of the preceding resonances is 9 : 1 : 60 : 30. (*c*) At this stage in this new experiment the ratio of the preceding resonances is 25 : 42 : 9 : 24. (*d*) At this stage the ratio of the preceding resonances is 4 : 4 : 31 : 61.

20 M. Otto, Diplom Thesis, University of Erlangen-Nürnberg, 2000.

21 J. Drabowicz, B. Dudziński, M. Mikołajczyk, M. W. Wieczorek and W. R. Majzner, *Tetrahedron*: *Asymmetry*, 1998, **9**, 1171.

22 M. A. Dewey, Y. Zhou, Y. Liu and J. A. Gladysz, *Organometallics*, 1993, **12**, 3924.

23 D. M. Dalton, J. M. Fernández, K. Emerson, R. D. Larsen, A. M. Arif and J. A. Gladysz, *J. Am. Chem. Soc.*, 1990, **112**, 9198.

24 M. K. Smith, J. A. Gibson, C. G. Young, J. A. Broomhead, P. C. Junk and F. R. Keene, *Eur. J. Inorg. Chem.*, 2000, 1365.

25 R. W. Murray, *Chem. Rev.*, 1989, **89**, 1187; W. Adam, R. Curci and J. O. Edwards, *Acc. Chem. Res.*, 1989, **22**, 205.

26 Representative examples: W. A. Schenk, J. Frisch, W. Adam and F. Prechtl, *Inorg. Chem.*, 1992, **31**, 3329; M. C. Fermin and J. W. Bruno, *J. Am. Chem. Soc.*, 1993, **115**, 7511; S. L. Griffiths, S. Perrio and S. E. Thomas, *Tetrahedron*: *Asymmetry*, 1994, **5**, 1847; S. Sun, J. O. Edwards, D. A. Sweigart, L. D'Accolti and R. Curci, *Organometallics*, 1995, **14**, 1545.

27 (*a*) I. Saura-Llamas and J. A. Gladysz, *J. Am. Chem. Soc.*, 1992, **114**, 2136; (*b*) M. A. Dewey, G. A. Stark and J. A. Gladysz, *Organometallics*, 1996, **15**, 4798.

28 Y. Ducommun, L. Helm, A. E. Merbach, B. Hellquist and L. I. Elding, *Inorg. Chem.*, 1989, **28**, 377.

29 Examples containing both oxygen- and sulfur-bound DMSO: A. Mercer and J. Trotter, *J. Chem. Soc.*, *Dalton Trans.*, 1975, 2480; V. I. Sokol and M. A. Porai-Koshits, *Koord. Khim.*, 1975, **1**, 577; A. R. Davies, F. W. B. Einstein, N. P. Farrell, B. R. James and R. S. McMillan, *Inorg. Chem.*, 1978, **17**, 1965; L. I. Elding and Å Oskarsson, *Inorg. Chim. Acta*, 1987, **130**, 209; W. M. Attia and M. Calligaris, *Acta Crystallogr.*, *Sect C*, 1987, **43**, 1426; E. Alessio, G. Mestroni, G. Nardin, W. M. Attia, M. Calligaris, G. Sava and G. Zorzet, *Inorg. Chem.*, 1988, **27**, 4099; D. P. Bancroft, F. A. Cotton and M. Verbruggen, *Acta Crystallogr.*, *Sect. C*, 1989, **45**, 1289; M. Calligaris, P. Faleschini and E. Alessio, *Acta Crystallogr.*, *Sect. C*, 1991, **47**, 747; E. Alessio, G. Balducci, M. Calligaris, W. M. Attia and G. Mestroni, *Inorg. Chem.*, 1991, **30**, 609; E. Alessio, B. Milani, M. Bolle, G. Mestroni, P. Faleschini, F. Todone, S. Geremia and M. Calligaris, *Inorg. Chem.*, 1995, **34**, 4722.

30 M. Calligaris, P. Faleschini, F. Todone, E. Alessio and S. Geremia, *J. Chem. Soc.*, *Dalton Trans.*, 1995, 1653.

31 N. Quirós Méndez, C. L. Mayne and J. A. Gladysz, *Angew. Chem.*, *Int. Ed. Engl.*, 1990, **29**, 1475; N. Quirós Méndez, C. L. Mayne and J. A. Gladysz, *Angew. Chem.*, 1990, **102**, 1509.

32 T.-S. Peng and J. A. Gladysz, *J. Am. Chem. Soc.*, 1992, **114**, 4174.

33 Y. Wang, F. Agbossou, D. M. Dalton, Y. Liu, A. M. Arif and J. A. Gladysz, *Organometallics*, 1993, **12**, 2699.

34 Interestingly, 1 : 1 DMSO adducts of closely related chloropalladium bipyridine and ethylenediamine fragments crystallize as oxygen-bound and sulfur-bound isomers, respectively: G. Annibale, L. Cattalini, V. Bertolasi, V. Ferretti, G. Gilli and M. L. Tobe, *J. Chem. Soc.*, *Dalton Trans.*, 1989, 1265.

35 N. Quirós Méndez, J. W. Seyler, A. M. Arif and J. A. Gladysz, *J. Am. Chem. Soc.*, 1993, **115**, 2323.

36 C. H. Winter, W. R. Veal, C. M. Garner, A. M. Arif and J. A. Gladysz, *J. Am. Chem. Soc.*, 1989, **111**, 4766; see also C. H. Winter, A. M. Arif and J. A. Gladysz, *Organometallics*, 1989, **8**, 219.

37 T.-S. Peng, A. M. Arif and J. A. Gladysz, *J. Chem. Soc.*, *Dalton Trans.* 1995, 1857.

38 G. L. Crocco, K. E. Lee and J. A. Gladysz, *Organometallics*, 1990, **9**, 2819.

39 E. L. Clennan and K. Yang, *J. Org. Chem.*, 1993, **58**, 4504.

40 For a specialized but interesting diastereoselective air oxidation of a chiral sulfide complex to an oxygen-bound sulfoxide complex see A. Berkessel, M. Bolte and T. Schwenkreis, *J. Chem. Soc.*, *Chem. Commun.*, 1995, 535.

41 N. J. Leonard and C. R. Johnson, *J. Org. Chem.*, 1962, **27**, 282.

42 R. W. Murray and R. Jeyaraman, *J. Org. Chem.*, 1985, **50**, 2847; W. Adam, J. Bialas and L. Hadjiarapoglou, *Chem. Ber.*, 1991, **124**, 2377.

43 J. M. Fernández and J. A. Gladysz, *Organometallics*, 1989, **8**, 207; C. R. Jablonski, *Aldrich. Acta*, 1990, **23**, 58.

44 F. Agbossou, E. J. O'Connor, C. M. Garner, N. Quirós Méndez, J. M. Fernández, A. T. Patton, J. A. Ramsden and J. A. Gladysz, *Inorg. Synth.*, 1992, **29**, 211.

45 Diastereomer ratios of sulfoxide complexes are summarized in Scheme 1.

46 IR spectra were recorded as thin films.

47 NMR data for sulfoxide and sulfide complexes that differ from those in Table 1 or reference 7 only in the counter anion are given in ESI (all measurements used the conditions in Table 1).

48 B. A. Frenz, The Enraf-Nonius CAD 4 SDP, A Real-time System for Concurrent X-ray Data Collection and Crystal Structure Determination, in *Computing and Crystallography*, eds. H. Schenk, R. Olthof-Hazelkamp, H. von Konigsveld and G. C. Bassi, Delft University Press, Delft, 1978, pp. 64–71.

49 D. T. Cromer and J. T. Waber, in *International Tables for X-ray Crystallography*, eds. J. A. Ibers and W. C. Hamilton, Kynoch Press, Birmingham, 1974, vol. IV, pp. 72–98, 149, 150, tables 2.2B and 2.3.1.